Butyrate increases methylglyoxal production through regulation of the JAK2/Stat3/Nrf2/Glo1 pathway in castration-resistant prostate cancer cells

YI-JAN HSIA[1], ZHANG-MIN LIN[2], TAOLAN ZHANG[3-5] and TZ-CHONG CHOU[2,6-8]

[1]Dental Department and Division of Oral and Maxillofacial Surgery, Taipei Tzu Chi Hospital, Buddhist Tzu Chi Medical Foundation, New Taipei 23142; [2]Cathay Medical Research Institute, Cathay General Hospital, New Taipei 22174, Taiwan, R.O.C.; [3]The First Affiliated Hospital, Department of Pharmacy; [4]School of Pharmacy; [5]The First Affiliated Hospital, Chinese Traditional Medicine Research Platform of Major Epidemic Treatment Base, Hengyang Medical School, University of South China, Hengyang, Hunan 421001, P.R. China; [6]Graduate Institute of Medical Sciences, National Defense Medical Center, Taipei 11490; [7]Department of Pharmacology, National Defense Medical Center, Taipei 11490; [8]China Medical University Hospital, China Medical University, Taichung 40400, Taiwan, R.O.C.

Received June 29, 2023; Accepted February 23, 2024

DOI: 10.3892/or.2024.8730

Abstract. Cancer cells are characterized by increased glycolysis, known as the Warburg effect, which leads to increased production of cytotoxic methylglyoxal (MGO) and apoptotic cell death. Cancer cells often activate the protective nuclear factor erythroid 2-related factor2 (Nrf2)/glyoxalase1 (Glo1) system to detoxify MGO. The effects of sodium butyrate (NaB), a product of gut microbiota, on Nrf2/Glos/MGO pathway and the underlying mechanisms in prostate cancer (PCa) cells were investigated in the present study. Treatment with NaB induced the cell death and reduced the proliferation of PCa cells (DU145 and LNCap). Moreover, the protein kinase RNA-like endoplasmic reticulum kinase/Nrf2/Glo1 pathway was greatly inhibited by NaB, thereby accumulating MGO-derived adduct hydroimidazolone (MG-H1). In response to a high amount of MGO, the expression of Nrf2 and Glo1 was attenuated, coinciding with an increased cellular death. NaB also markedly inhibited the Janus kinase 2 (JAK2)/Signal transducer and activator of transcription 3 (Stat3) pathway. Conversely, co-treatment with Colivelin, a Stat3 activator, significantly reversed the effects of NaB on Glo1 expression, MG-H1 production, and the cell migration and viability. As expected, overexpression of Stat3 or Glo1 reduced NaB-induced cell death. The activation of calcium/calmodulin dependent protein kinase II gamma and reactive oxygen species production also contributed to the anticancer effect of NaB. The present study, for the first time, demonstrated that NaB greatly increases MGO production through suppression of the JAK2/Stat3/Nrf2/Glo1 pathway in DU145 cells, a cell line mimicking castration-resistant PCa (CRPC), suggesting that NaB may be a potential agent for PCa therapy.

Correspondence to: Professor Tz-Chong Chou, Cathay Medical Research Institute, Cathay General Hospital, Lane 160, 32 Jiancheng Road, New Taipei 22174, Taiwan, R.O.C.
E-mail: chou195966@gmail.com

Key words: butyrate, methylglyoxal, glyoxalases, nuclear factor erythroid 2-related factor2, signal transducer and activator of transcription 3, prostate cancer

Introduction

Prostate cancer (PCa) is a prevalent malignancy and is a major cause of cancer-related death in men (1). It is estimated that despite therapeutic advancements, the global mortality rate of PCa will double from 2018 to 2040. There are two types of PCa cells, including androgen-independent human PCa cell lines (DU145, PC3) and androgen-sensitive human PCa cell line (LNCap). The DU145 cells are commonly used as an *in vitro* model for castration-resistant PCa (CRPC) research. By contrast, LNCap cells exhibit a comparatively slow growth rate, and are commonly used as an *in vitro* model for the early-stage and androgen-sensitive PCa. Despite the progress in the treatment, the outcome for patients with CRPC remains poor with a relatively short overall survival; it remains a formidable challenge in CRPC therapy. Therefore, there is an urgent need to further understand the pathogenic mechanisms of PCa, particularly CRPC, and subsequently develop more effective strategies and agents to counteract PCa progression.

Tumors prefer to using aerobic glycolysis (Warburg effect), a hallmark of cancer cells, to metabolize glucose and generate energy and materials to sustain the rapid growth of tumors (2). Increased glycolytic flux leads to the production of a high amount of cytotoxic methylglyoxal (MGO), a byproduct of glycolysis. MGO also serves as a potent glycating agent and ultimately causes glycative stress. MGO can rapidly react with

proteins or lipids to generate advanced glycation end-products (AGEs). The hydroimidazolone (MG-H1) is a major product from MGO-derived AGEs and it can induce cell damage and apoptosis (3). A substantial increase in MGO generation in PCa has been confirmed to impede cell cycle progression and the glycolytic pathway and thus induces apoptosis (4). MGO can be detoxified by the enzymes glyoxalases (Glos) comprising glyoxalase 1 (Glo1) and glyoxalase 2 (Glo2), to D-lactate, a surrogate marker of MGO production, thus facilitating cell survival (5). The overexpression and elevated activity of Glo1 has been documented in various human cancers, including PCa; it is also closely linked to cancer aggressiveness, progression and resistance to drugs (6,7). These findings highlighted the survival-promoting effect of Glo1 in tumors. Therefore, modulating the Glo1/MGO pathway may be a promising strategy to attenuate the progression of PCa.

Nuclear factor erythroid 2-related factor 2 (Nrf2), a key transcription factor, is able to activate the transcription of several protective genes involved in cell survival and antioxidant defense. However, prolonged activation of Nrf2 is considered to have a risk of promoting oncogenesis by promoting cancer growth, metastasis, metabolic reprogramming and resistance to therapeutic interventions (8,9). Importantly, Nrf2 also induces Glo1 expression and activity (10). Hence, suppressing Nrf2/Glo1-dependent detoxification system, resulting in excessive production of toxic MGO, is a feasible strategy for the treatment of cancer, particularly in tumors with Glo1 overexpression that heavily rely on Glo1-dependent processes. A variety of mediators and signaling pathways have been reported to control the expression and activity of Nrf2 and Glo1. Under hypoxia and oxidative stress, the functions of the endoplasmic reticulum (ER) are disrupted and consequently the misfolded proteins accumulate within the ER lumen, thereby inducing ER stress and initiating the unfolded protein response (11). Nrf2 is a direct substrate of protein kinase RNA-like ER kinase (PERK), one of the ER stress sensor proteins (12). Moreover, PERK-dependent phosphorylation of Nrf2 results in the nuclear translocation and activation of Nrf2 (13).

Signal transducer and activator of transcription 3 (Stat3), a member of the Stat family, is a multifunctional transcription factor. Activation of Stat3 promotes cancer growth, metastasis, angiogenesis and the resistance to apoptosis (14). One recent study indicated that Stat3 and Nrf2 can activate and interact with each other to promote tumorigenesis (15). The participation of reactive oxygen species (ROS) in numerous cell signaling pathways and cellular processes, including apoptosis, is well known. With their ability to inhibit the activity of Glo1 and trigger apoptotic cell death (16), ROS may be a potential target for the regulation of the Glo1/MGO pathway. The ER stress-mediated calcium release from ER activates calcium/calmodulin-dependent protein kinase II (CaMKII), which acts as a link between metabolic reprogramming and the initiation of apoptosis (17). The aberrant expression and activity of CaMKII are commonly observed in various tumors, potentially being an important factor driving cancer progression (18). Collectively, inhibition of the Nrf2/Glo1 pathway, leading to MGO production through regulation of various signaling pathways and tumorigenic genes represents a promising approach for PCa therapy.

Butyrate, a short-chain fatty acid, is produced by specific gut microbiota via the fermentation of dietary fiber and carbohydrates. Numerous studies have demonstrated that sodium butyrate (NaB) exhibits a variety of benefits, including anticancer activity (19,20). However, the effects of NaB on the Nrf2/Glo1/MGO pathway and the molecular mechanisms involved in PCa cells remain unexplored, and this area deserves further investigation.

Materials and methods

Reagents. MGO, NaB and AI-1 were purchased from Sigma-Aldrich; Merck KGaA. N-acetyl-cysteine (NAC), Colivelin, cct020312 and ruxolitinib were purchased from MedChemExpress. KN-93 was purchased from Selleck Chemicals. DCFDA was purchased from Abcam. Referring to previous studies (21-27), the concentrations of these agents used in the present study were chosen.

Cell culture. The DU145 (cat. no. 60348), LNCaP (cat. no. 60088) were purchased from Bioresource Collection and Research Center (Hsinchu, Taiwan) and human prostate epithelial cells (RWPE-1; cat. no. CRL-3607) was purchased from American Type Culture Collection. The cells were cultured in RPMI-1640 medium (cat. no. 23400-021; Thermo Fisher Scientific, Inc.) supplemented with 10% fetal bovine serum (cat. no. SH30396.03; Cytiva) and maintained in humidified atmosphere of 5% CO_2 at 37˚C. The RWPE-1 cells are cultured in in keratinocyte serum-free medium (cat. no. 17005042; Thermo Fisher Scientific, Inc.) supplemented with bovine pituitary extract and epidermal growth factor.

Cell proliferation and viability. After cells (8,000 cells per well) were treated with various agents for 24 or 48 h, 10 μl of the reagent of Cell Counting Kit-8 (cat. no. HY-K0301; MedChemExpress) was added into each well with 1:10 diluted in medium and incubated for another 1 h at 37˚C. Then, the absorbance was measured at 450 nm with a microplate reader (BioTek Instruments, Inc.).

Cell fractionation. The nuclear/cytosol fractionation kit (cat. no. ab289882; Abcam) was used to separate nuclear and cytoplasmic proteins according to manufacturer's instruction.

Immunofluorescence assay. Cells attached on μ-Slide 8 well (Ibidi GmbH) were treated with NaB for 24 h followed by a fixation with 10% formalin at room temperature for 10 min. The non-specific binding sites were blocked with 1% BSA (cat. no. APL-0017; APOLO Biochemical; Group Research Tech. Inc.) in PBS at room temperature for 1 h. Then, the cells were incubated with anti-Nrf2 antibody (1:200 in 1% BSA in PBS) at 4˚C for overnight, and DyLight 488 conjugated secondary antibody (1:500 in 1% BSA in PBS) was added at 4˚C for 1 h. After washing with PBS, the nuclei of cells were stained with Hoechst 33342 at room temperature for 1 min. Images of the slides were captured with a fluorescence microscope (Olympus IX73; Olympus Corp.).

Western blotting. The cells were harvested with RIPA lysis buffer (cat. no. 89900; Thermo Fisher Scientific, Inc.) supplemented with protease and phosphatase inhibitors. The protein amount of lysate was determined by using BCA assay kit

Table I. List of antibodies.

Primary antibody	Manufacturer	Cat. no.
α-tubulin	Croyez Bioscience Co., Ltd.	C06002
β-actin	Proteintech Group, Inc.	66009-1-Ig
BTB domain and CNC homolog 1	Taiclone Biotech Corp.	tcea18686
c-Myc	GeneTex, Inc.	GTX103436
CaMKII	Abcam	ab92332
p-CaMKII (T286/T287)	Cell Signaling Technology, Inc.	12716
Caspase 9	Cell Signaling Technology, Inc.	9508
Cyclin D1	Cell Signaling Technology, Inc.	2978
ERK	Cell Signaling Technology, Inc.	9102
p-ERK (T202/Y204)	Cell Signaling Technology, Inc.	9101
GAPDH	Proteintech Group, Inc.	60004-1-Ig
Glo1	Proteintech Group, Inc.	15140-1-AP
Glo2	Proteintech Group, Inc.	17196-1-AP
Heme oxygenase-1	Abcam	AB13248
JAK2	Cell Signaling Technology, Inc.	3230
p-JAK2 (Y1007/Y1008)	Cell Signaling Technology, Inc.	3771
JNK	Arigo Biolaboratories Corp.	ARG51218
p-JNK (T183/T185 for JNK1/2, T221/223 for JNK3)	Arigo Biolaboratories Corp.	ARG51807
Lamin B1	ABclonal Biotech Co., Ltd.	A16909
Nuclear factor erythroid 2-related factor 2	ABclonal Biotech Co., Ltd.	A1244
p38	Cell Signaling Technology, Inc.	9212
p-p38 (T180/Y182)	Cell Signaling Technology, Inc.	9211
Poly(ADP-Ribose) Polymerase 1	Cell Signaling Technology, Inc.	9532
PERK	GeneTex, Inc.	GTX129275
p-PERK (S555)	GeneTex, Inc.	GTX00673
Stat1	Cell Signaling Technology, Inc.	9172
p-Stat1 (S727)	GeneTex, Inc.	GTX132507
Stat3	Cell Signaling Technology, Inc.	4904
p-Stat3 (Y705)	Cell Signaling Technology, Inc.	9145
Vinculin	GeneTex, Inc.	GTX113294
Secondary antibody	Manufacturer	Cat. no.
Goat anti-Rabbit IgG HRP	GeneTex, Inc.	GTX213110-01
Goat anti-Mouse IgG HRP	GeneTex, Inc.	GTX213111-01
Goat anti-Rabbit IgG DyLight488	GeneTex, Inc.	GTX213110-04

CaMKII, calcium/calmodulin dependent protein kinase II gamma; p-, phosphorylated; Glo, glyoxalase; JAK2, Janus kinase 2; PERK, eukaryotic translation initiation factor 2 alpha kinase 3; Stat, signal transducer and activator of transcription.

(cat. no. 23225; Thermo Fisher Scientific, Inc.), and the lysate was mixed with 1X Laemmli dye and beta-mercaptoethanol. The protein of lysate (10 μg) was loaded per lane and resolved with 7.5 or 10% SDS-PAGE, which was subsequently transferred onto polyvinylidene difluoride membrane. The transblotted membranes were blocked with 5% non-fat milk in TBS with 0.1% Tween-20 (v/v) (TBST) for 1 h at room temperature. After washing with TBST, the membranes were incubated with target primary antibody at 4˚C for overnight. Then, the membranes were rinsed three times with TBST and incubated with horseradish peroxidase (HRP)-conjugated secondary antibody for 1 h at room temperature. The immunoreactive bands were detected by a chemiluminescent kit (PerkinElmer, Inc.) and visualized using MultiGel-21 (TOPBIO). The relative density of protein bands was determined by ImageJ 1.53V software (National Institutes of Health) The vinculin or α-tubulin was used as internal loading control. Relative information of the primary antibodies used in the present study is included in Table I.

Cell apoptosis analysis by flow cytometry. For apoptosis assay, cells (10^5) were incubated with FITC-Annexin V and 7-AAD (BD Biosciences) at 4˚C for 30 min in the dark and analyzed using a flow cytometer (FACSCalibur; BD Biosciences). The percentage of apoptotic cells was determined by the software CellQuest™ Pro (BD biosciences).

Overexpression plasmid transfection. Transfection complex was prepared using TransIT-X2 (Mirus Bio, LLC). The mass

of the overexpression plasmids used was as follows: 1.8 μg DNA per well for 96 well, 4.8 μg DNA per well for 12 well. The DU145 cells were transfected with pCMV2 control vector (CV013), pCMV2-Stat3-Myc (HG10034-CM), or pCMV2-Glo1-HA (HG12223-CY) (Sino Biological, Inc.) at 37˚C for 24 h according to the manufacturer's protocol. Then, NaB was added for 48 h to perform subsequent tests.

MGH1 and D-lactate measurement. The amount of MGO was determined by measuring its major adduct MG-H1, using OxiSelectTM Methylgloxal ELISA kit (cat. no. ab238543; Abcam) according to manufacturer's instruction. Briefly, at the end of the treatment, cells were lysed with RIPA lysis buffer. Then 10 μl of lysate was loaded into MGO-conjugate coated plate and incubated with MGO-antibody at room temperature for 1 h followed by washing with wash buffer. Secondary antibody was added and incubated at room temperature for 1 h. Finally, the substrate of HRP was added, and the absorbance of 450 nm was measured using a microplate reader (BioTek Instruments, Inc.). The intracellular D-Lactate was measured by D-Lactate assay kit (ab83429, Abcam). Briefly, the cells were lysed and collected the supernatants after centrifugation (12,000 x g at 4˚C for 15 min) for determining the production of intracellular D-lactate by measuring the absorbance at 450 nm.

Intracellular ROS measurement. After cells were treated with agents for 48 h, 10 μM of DCFDA (cat. no. ab273640; Abcam) dissolved in medium was added followed by incubation for 1 h at 37˚C. The fluorescence intensity was measured using CLARIOstar Plus (BMG Labtech GmbH) (Ex/Em=495/529 nm).

Statistical analysis. All data were obtained from at least three experiments. The results were expressed as the mean ± SEM. The difference between groups was analyzed by one-way ANOVA and Bonferroni post hoc test using statistical software SigmaPlot 12.0 (Grafiti). $P<0.05$ was considered to indicate a statistically significant difference.

Results

Effects of NaB on the cell viability, proliferation, Nrf2/Glos cascade and the production of D-lactate and MG-H1 in PCa cells. Treatment with NaB dose-dependently attenuated the cell viability and proliferation of DU145 and LNCaP cells (Fig. 1A). NaB significantly inhibited the expression of Nrf2, Glo1 and heme oxygenase-1 (HO-1), a downstream gene of Nrf2, without affecting the Glo2 expression, as well as the production of D-lactate, but increased MG-H1 formation in both cell lines (Fig. 1B and C). These results indicated that the effects of NaB were similar on the Nrf2/Glo1/MGO pathway in DU145 and LNCaP cells. Of note, significant therapeutic challenges still persist in CRPC due to the resistance to current treatments. Thus, in the subsequent mechanistic investigations, DU145 cells were selected as the primary cell line that mimics CRPC, to gain deeper insights into the pathogenesis of CRPC.

Effects of NaB on PERK and Nrf2 activation. The activity of Nrf2 can be induced by PERK activation via ER stress (12). As demonstrated in Fig. 2A, NaB treatment significantly inhibited PERK phosphorylation in DU145 cells. By contrast, co-treatment with cct020312, an activator of PERK, elevated Nrf2 expression and cell viability compared with NaB-treated cells (Fig. 2B), suggesting the involvement of PERK in NaB-mediated Nrf2 expression and apoptosis. The nuclear translocation of Nrf2 is required for its transcriptional activity. Conversely, nuclear BTB domain and CNC homolog 1 (Bach1) compete with the binding of Nrf2 to antioxidant response element (ARE), thereby inhibiting the transcriptional activity of Nrf2 (28). NaB treatment markedly reduced the nuclear level of Nrf2, while the nuclear level of Bach1 was increased (Fig. 2C). Immunofluorescence assay also revealed similar change in nuclear level of Nrf2 in NaB-treated DU145 cells (Fig. 2D). Therefore, inhibition of the protein expression and activity of Nrf2 by NaB may be associated with PERK inactivation and accumulation of nuclear Bach1. Then, AI-1, an activator of Nrf2, was added to assess the role of Nrf2 on NaB-regulated Glo1 expression. Co-treatment with AI-1 and NaB significantly attenuated the downregulation of Glo1 expression by NaB (Fig. 2E), indicating Nrf2 as a stimulator of Glo1 expression in NaB-treated DU145 cells. Interestingly, AI-1 treatment alone did not affect Glo1 expression compared with the control group, suggesting that Nrf2 may be not involved in the Glo1 expression of untreated cells.

Effects of Stat3 on NaB-mediated Glo1 expression. It is known that activation of the Janus kinase 2 (JAK2)/Stat3 pathway promotes cancer progression (14). Conversely, signal transducer and activator of transcription 1 (Stat1) exerts a tumor-suppressing activity (29). Treatment with NaB significantly inhibited JAK2 and Stat3 phosphorylation, but increased Stat1 phosphorylation (Fig. 3A). Ruxolitinib, an inhibitor of JAK2, significantly reduced the phosphorylation of Stat3 and Glo1 expression, suggesting that inhibition of JAK2 activity contributes to the attenuation of Stat3 activation and Glo1 expression by NaB (Fig. 3B). NaB treatment also significantly increased ROS production (Fig. 3C). When ROS production was abolished by NAC, a free radical scavenger, NaB-mediated inhibition of p-Stat3 was significantly counteracted (Fig. 3D). Thus, inhibiting JAK2 activity and elevating ROS production may account for NaB-mediated inactivation of Stat3. Moreover, NaB-mediated downregulation of Glo1 and HO-1 and enhanced production of MG-H1 by NaB were significantly reversed by Colivelin, a Stat3 activator (Fig. 3E and F). Collectively, the inhibitory effect of NaB on the Glo1/MGO cascade may be due to suppression of Stat3 activity via elevation of ROS production.

Effects of MGO on the expression of Nrf2, Glo1 and HO-1. Overproduction of MGO resulting from the downregulation of Glo1 induces apoptosis and inhibits the proliferation and invasion of breast cancer cells (30). The protein levels of Nrf2, Glo1 and HO-1 were unchanged after treatment with low MGO concentrations (0.2 and 0.4 mM). At high MGO concentrations (0.8 and 1.6 mM), the protein expression levels of the aforementioned genes were significantly inhibited accompanied by a dose-dependent decrease in cell viability compared with that of the control group (Fig. 4A). These findings suggested that a feedback loop exists between MGO and the expression of

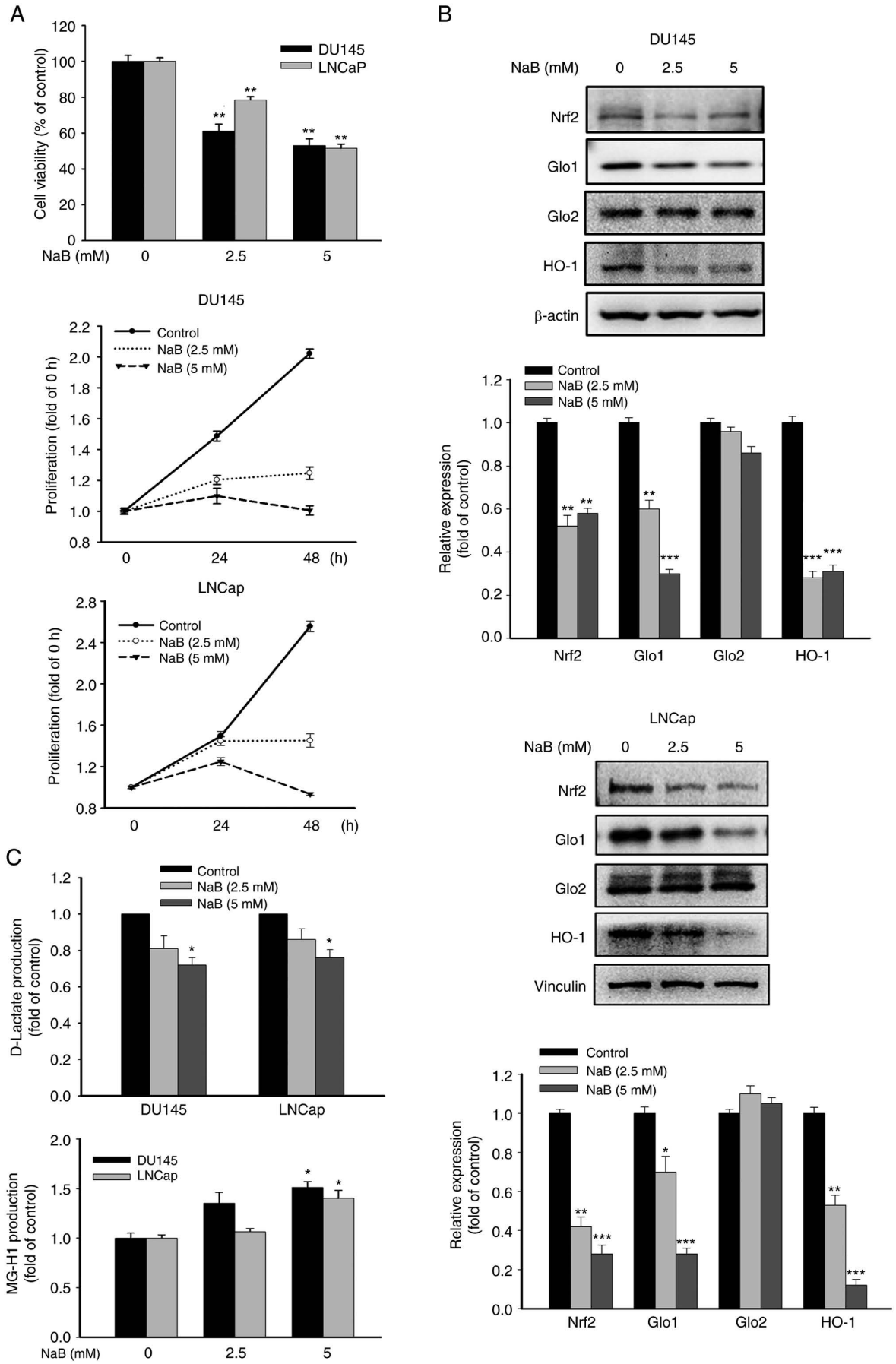

Figure 1. Effects of NaB on the cell viability, proliferation, Nrf2/Glos pathway in PCa cells. (A) The DU145 cells or LNCaP cell were treated with NaB (2.5 or 5 mM) for 48 h, the cell viability and proliferation, (B) the expression of target genes and (C) the production of D-lactate and MG-H1 were determined. Results are expressed as the mean ± SEM. *P<0.05, **P<0.01 and ***P<0.001 vs. the Control group. NaB, sodium butyrate; Nrf2, Nuclear factor erythroid 2-related factor 2; Glos, glyoxalases; PCa, prostate cancer; MG-H1, hydroimidazolone; HO-1, heme oxygenase-1.

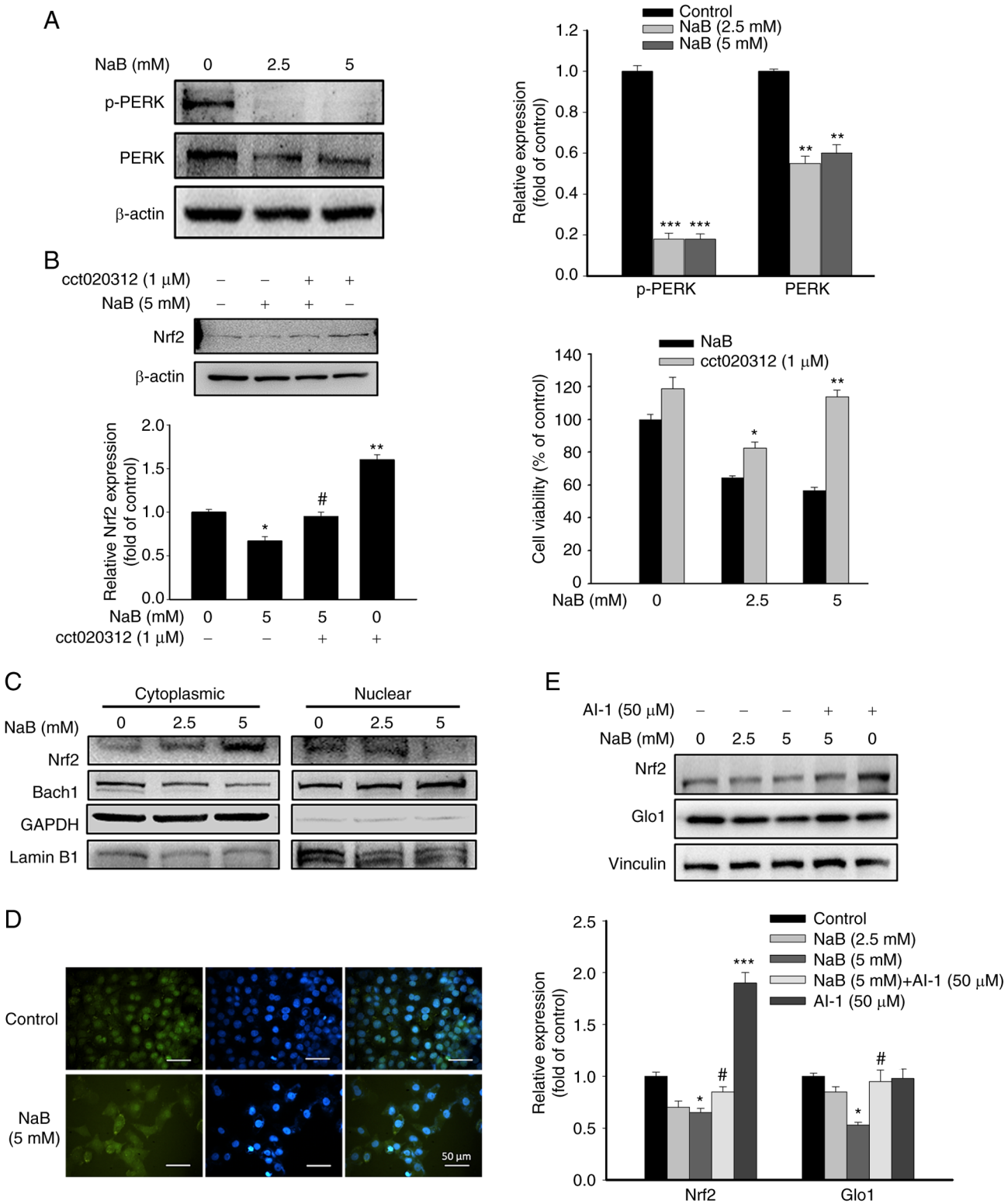

Figure 2. The effects of NaB on the activation of PERK and Nrf2. (A) DU145 cells were treated with NaB (2.5 or 5 mM) for 48 h, the PERK expression was determined. (B) The changes of Nrf2 expression and the cell viability were examined in cct020312 and NaB-treated cells. (C) After the cells treated with NaB for 24 h, the levels of cytoplasmic and nuclear Nrf2 and Bach1 were determined. (D) The distribution of Nrf2 in cytoplasm and nuclei in DU145 cells was evaluated by immunofluorescence assay. (E) The DU145 cells were incubated with AI-1 (50 μM) for 2 h followed by treatment with NaB for another 48 h, then the expression of Nrf2 and Glo1 was determined. Results are expressed as the mean ± SEM. *P<0.05, **P<0.01 and ***P<0.001 vs. the Control group; $^{\#}$P<0.05 vs. respective NaB-treated alone cells. NaB, sodium butyrate; PERK, eukaryotic translation initiation factor 2 alpha kinase 3; Nrf2, nuclear factor erythroid 2-related factor 2; Bach1, BTB domain and CNC homolog 1; Glo1, glyoxalase1.

Nrf2, Glo1 and HO-1 in DU145 cells, which further diminishes the MGO detoxifying system and induces cell death. The DU145 cells with overexpressed Glo1 or Stat3 were used to clarify their effects on the pro-apoptotic effect of NaB. It was revealed that overexpression of Glo1 or Stat3 reversed the decreased cell viability by NaB (Fig. 4B), supporting that

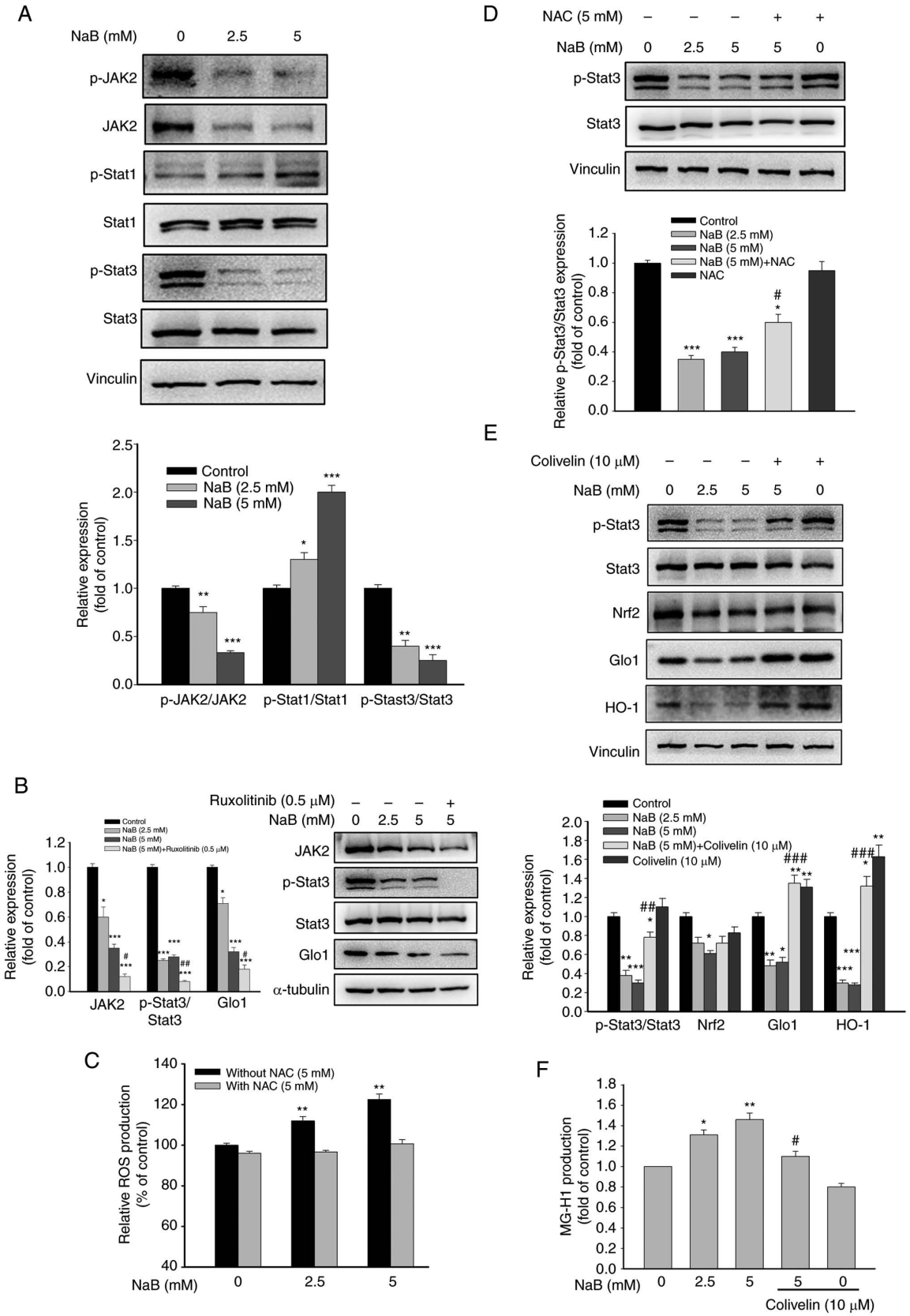

Figure 3. The effects of NaB on Stat1, JAK2 and Stat3 expression. (A) DU145 cells were treated with NaB (2.5 or 5 mM) for 48 h and the expression of these genes was determined. (B) The DU145 cells were incubated with ruxolitinib (0.5 μM) for 2 h followed by treatment with NaB for 48 h, the expression of p-Stat3 and Glo1 was determined. (C) The relative ROS was measured in cells treated with NaB (2.5 or 5 mM) for 48 h. (D) After the cells were incubated with NAC (5 mM) or medium for 2 h followed by treatment with NaB for another 48 h, the protein level of p-Stat3 was determined in various groups. (E and F) Cells were pretreated with Colivelin (10 μM) or medium for 2 h followed by treatment with NaB for another 48 h. Then, the expression of the (E) target genes and (F) MG-H1 production were determined. Results are expressed as the mean ± SEM. *P<0.05, **P<0.01 and ***P<0.001 vs. the Control group; $^{\#}$P<0.05, $^{\#\#}$P<0.01 and $^{\#\#\#}$P<0.001 vs. respective NaB-treated alone cells. NaB, sodium butyrate; Stat, signal transducer and activator of transcription; JAK2, Janus kinase 2; Glo1, glyoxalase1; ROS, reactive oxygen species; NAC, N-acetyl-cysteine; MG-H1, hydroimidazolone; Nrf2, nuclear factor erythroid 2-related factor 2; HO-1, heme oxygenase-1; p-, phosphorylated.

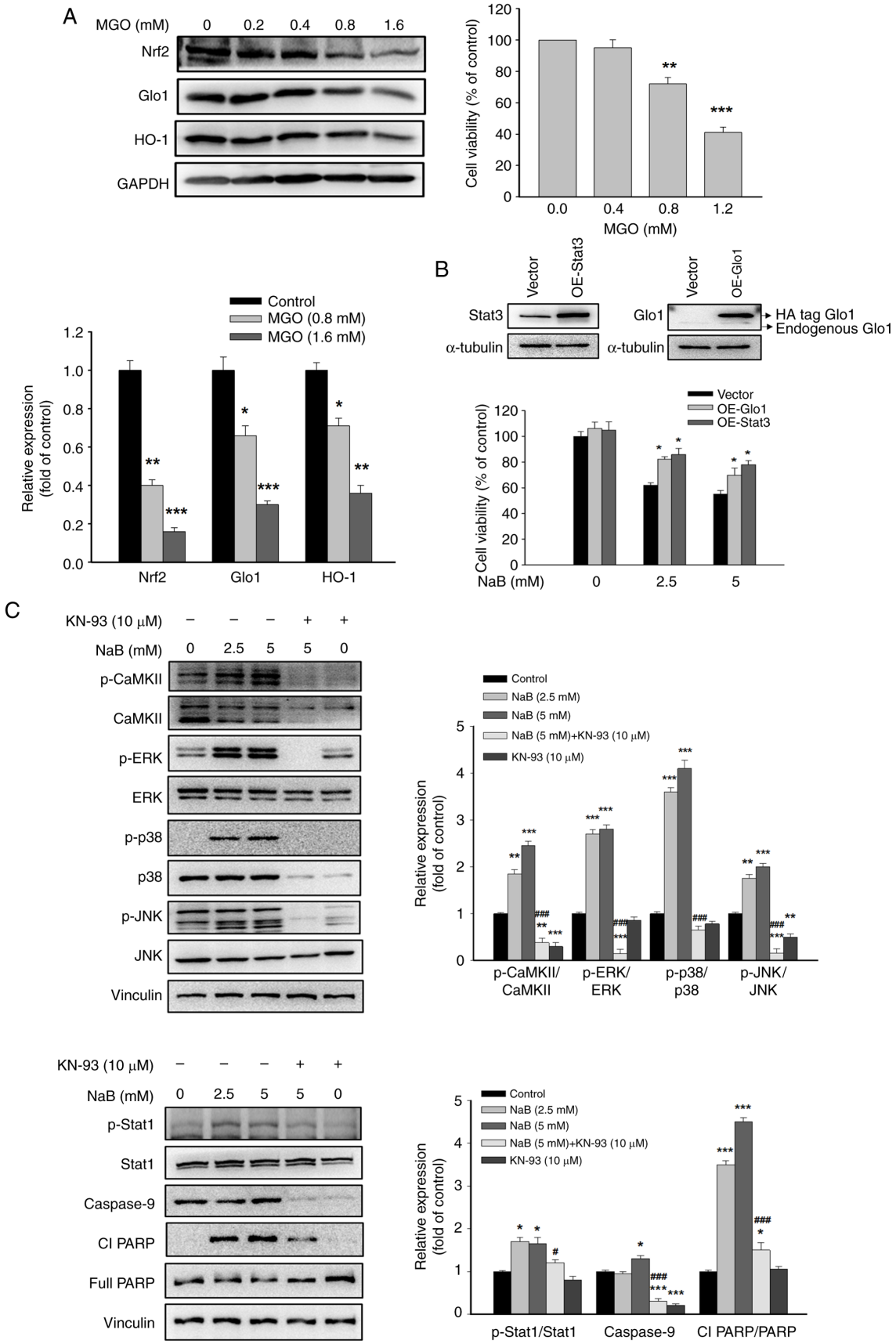

Figure 4. The effects of MGO, Glo1, Stat3 and CaMKII phosphorylation on NaB-mediated target gene expression and cell viability. (A) After treatment with MGO (0.2-1.6 mM) for 48 h, the expression of Nrf2, Glo1 and HO-1, as well as the cell viability were determined. (B) The cell viability of the DU145 cells with overexpression of Glo1 or Stat3 was examined. (C) Cells were pretreated with KN-93 (10 μM) for 2 h followed by treatment with NaB for 48 h. Then, the expression of MAPKs and pro-apoptotic proteins were determined. Results are expressed as mean ± SEM. *P<0.05, **P<0.01 and ***P<0.001 vs. the Vector or Control group; $^{\#}$P<0.05, $^{\#\#\#}$P<0.001 vs. respective NaB-treated alone cells. MGO, methylglyoxal; Glo1, glyoxalase1; Stat3, signal transducer and activator of transcription 3; CaMKII, calcium/calmodulin dependent protein kinase II gamma; NaB, sodium butyrate; Nrf2, nuclear factor erythroid 2-related factor 2; HO-1, heme oxygenase-1; PARP, Poly (ADP-Ribose) polymerase.

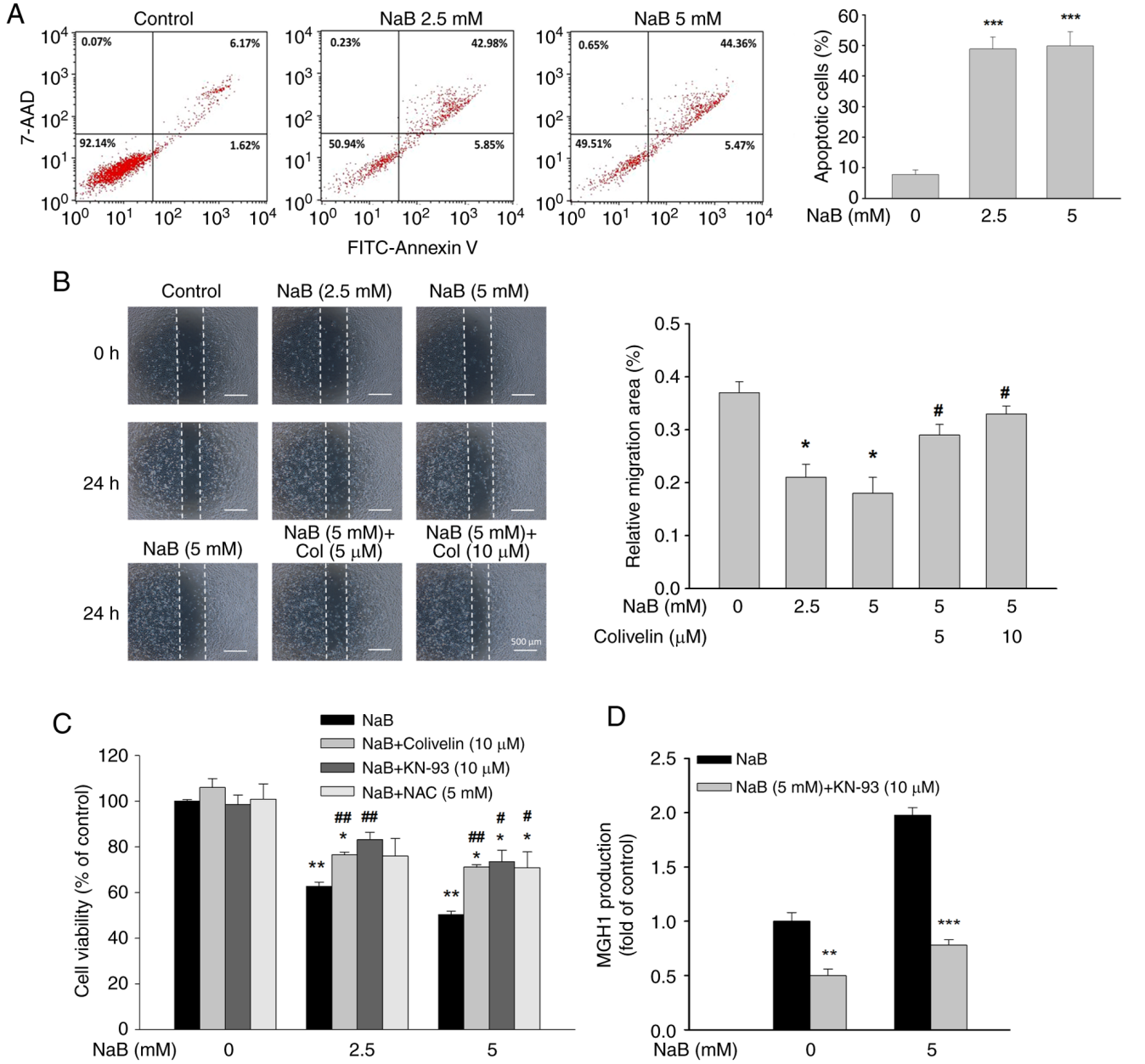

Figure 5. Effects of NaB on cell apoptosis and migration. After treatment with NaB (2.5 or 5 mM) for 48 h or indicated time, (A) the apoptotic cells (%), (B) the cell migration and (C) the cell viability in the presence or absence of Colivelin (10 μM), KN-93 (10 μM) or NAC (5 mM) for 48 h were examined in various groups. (D) The production of MG-H1 was measured. The cells were treated with KN-93 (10 μM) for 2 h followed by treatment with NaB for 48 h. Results are expressed as the mean ± SEM. *P<0.05, **P<0.01 and ***P<0.001 vs. the Control group; $^{\#}$P<0.05 and $^{\#\#}$P<0.01 vs. respective NaB-treated alone cells; NaB, sodium butyrate; NAC, N-acetyl-cysteine; MG-H1, hydroimidazolone; HO-1, heme oxygenase-1.

Stat3 and Glo1-dependent responses play important role in the anticancer activity of NaB in DU145 cells.

Effects of NaB on activation of CaMKII and MAPKs. As revealed in Fig. 4C, the phosphorylation of CaMKII, Stat1 and MAPKs, including JNK, ERK and p38, as well as the pro-apoptotic proteins, such as caspase 9 and cleaved Poly(ADP-Ribose) polymerase, were all significantly upregulated after NaB treatment. However, the effects of NaB were significantly abrogated by KN-93, a specific inhibitor of CaMKII, suggesting CaMKII as a key factor in the regulation of these genes.

Effects of NaB on apoptotic cell death and migration. Flow cytometric analysis revealed a significant increase in the percentage of early and late apoptotic cells in NaB-treated DU145 cells (Fig. 5A). In addition, NaB dose-dependently reduced the migration of DU145 cells, and this effect was significantly diminished by Colivelin (Fig. 5B). Co-treatment with Colivelin, KN-93, or NAC significantly reversed NaB-induced cell death (Fig. 5C). Accordingly, the cytotoxicity of NaB may be mediated by Stat3, CaMKII and ROS-dependent processes. Interestingly, KN-93 treatment greatly attenuated MG-H1 production irrespective of the absence or presence of NaB (Fig. 5D). Thus, it is possible that CaMKII-induced MGO production may at least in part contribute to NaB-induced apoptosis.

Effect of NaB on the proliferation and the viability of normal cells. The proliferation of DU145 cells and the expression

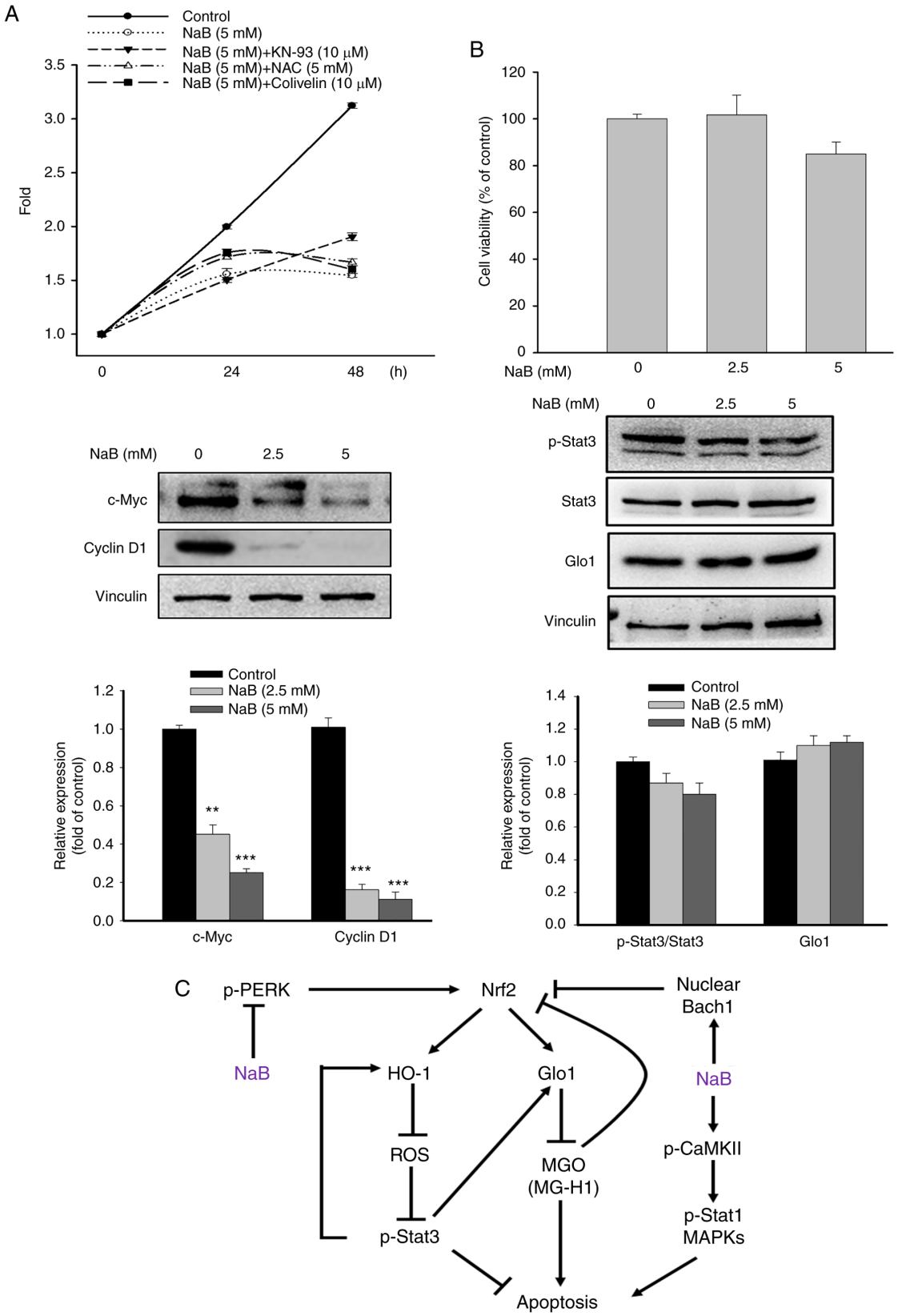

Figure 6. Effects of KN-93 on cell proliferation the effects of NaB on normal RWPE-1 cells. (A) The relative cell proliferation of DU145 cells and the expression of c-Myc and cyclin D1 were evaluated in NaB (5 mM) alone, and co-treatment with KN-93, NAC, or Colivelin for indicated time. (B) The cell viability and the levels of Glo1 and Stat3 in RWPE-1 cells were examined after treatment with NaB for 48 h. Results are expressed as the mean ± SEM. **P<0.01 and ***P<0.001 vs. the Control group. (C) The proposed schematic diagram of NaB-mediated Nrf2/Glo1/MGO pathway and apoptosis in PCa cells. NaB inhibits the expression and activity of Nrf2 through PERK inactivation and accumulation of nuclear Bach1. Then, Glo1expression is attenuated via suppression of Janus kinase 2/Stat3 pathway, leading to accumulation of MGO and apoptotic cell death. The elevated MGO further downregulates Nrf2, Glo1 and HO-1. The CaMKII-mediated activation of MAPKs and Stat1 also contributes to NaB-induced cell death. NaB, sodium butyrate; NAC, N-acetyl-cysteine; Glo1, glyoxalase1; Stat3, signal transducer and activator of transcription 3; Nrf2, nuclear factor erythroid 2-related factor 2; MGO, cytotoxic methylglyoxal; PERK, eukaryotic translation initiation factor 2 alpha kinase 3; Bach1, BTB domain and CNC homolog 1; HO-1, heme oxygenase-1; CaMKII, calcium/calmodulin dependent protein kinase II gamma.

of c-Myc and cyclin D1, the key mediators promoting cell proliferation (31), were significantly inhibited after NaB (5 mM) treatment for 48 h (Fig. 6A). Interestingly, compared with NaB-treated cells, only KN-93 slightly increased the cell proliferation at 48 h, while NAC and Colivelin had no significant effect on the cell proliferation. Notably, treatment with NaB did not significantly affect the viability and the levels of Glo1 and Stat3 in human prostate epithelial cells (RWPE-1) (Fig. 6B), indicating that the actions of NaB are specific for PCa cells.

Discussion

Most cancer cells prefer to utilize glycolysis to sustain growth even under aerobic condition, leading to accumulation of the cytotoxic MGO production. Various cancers exhibit a significant increase in the expression and activity of Glo1, a crucial enzyme responsible for MGO degradation, indicating Glo1 as a tumor promoting protein. Nrf2 plays a key role in the activation of Glo1 expression and activity (10). Therefore, suppressing the Nrf2/Glo1/MGO pathway may be a feasible strategy to mitigate cancer progression. To the best of the authors' knowledge, in the present study it was first demonstrated that NaB can increase MGO production in PCa cells through downregulation of Nrf2 and Glo1 expression via inhibition of JAK2/Stat3 cascade.

Under normal conditions, Nrf2 is sequestered in the cytoplasm by Kelch-like ECH-associated protein 1 (Keap1), followed by Nrf2 degradation by the ubiquitin-proteasome system. However, under oxidative stress, Nrf2 dissociates from Keap1 and translocates into the nucleus, where it forms a heterodimer with small Maf and binds to the ARE, thereby activating the transcription of several protective genes, such as Glo1 and HO-1. By contrast, the nuclear Bach1 hinders the access of Nrf2 to the ARE (28). Thus, the balance between nuclear Nrf2 and Bach1 determines the transcriptional activity of Nrf2. An important discovery in the present study was that NaB could inhibit the transcriptional activity of Nrf2, as evidenced by decreased Nrf2 and increased Bach1 levels in the nucleus. As expected, a significant reduction in the Glo1 expression and D-lactate production accompanied by elevated production of MG-H1 in NaB-treated DU145 or LNCap cells, was observed. However, activation of Nrf2 with AI-1 significantly reversed the downregulated Glo1 expression by NaB, indicating that Nrf2 is a key gene contributing to Glo1 induction. As activation of PERK increases Nrf2 expression/activity, the inhibition of PERK activity by NaB may be a mechanism causing Nrf2 downregulation. This concept was supported by the results that the activation of PERK with cct020312 elevated Nrf2 expression and the viability of NaB-treated cells. These findings suggested that NaB-mediated inhibition of Nrf2 expression may, at least in part, attribute to PERK inactivation.

Stat3 is a crucial transcriptional factor promoting the metastasis and progression of PCa (32). Stat3 is activated through phosphorylation at Tyr705 residue by JAK2. The JAK2/p-Stat3 pathway is capable of enhancing the stability of the Nrf2 protein (33). NaB treatment markedly inhibited the phosphorylation of JAK2 and Stat3 (Tyr705) in DU145 cells. To date, whether the JAK2/Stat3 pathway affects the Glo1 expression and MG-H1 production in PCa cells remains unexplored. Then, the role of Stat3 on Nrf2/Glo1/MGO pathway was examined by using ruxolitinib or Colivelin. The levels of p-Stat3 and Glo1 were further reduced by addition of ruxolitinib compared with that of NaB-treated alone cells. Conversely, Colivelin strongly reversed the effects of NaB on Glo1 expression and MG-H1 production without affecting Nrf2 expression. These results indicated that the JAK2/Stat3 pathway plays a critical role in the regulation of the Glo1/MGO pathway. Although the exact mechanism involved remains unclear, it is proposed that Stat3-induced Glo1 transcription may be due to the direct binding of Stat3 to Glo1 promoter (34). The investigation of the impact of Stat3 and Glo1 on the anticancer properties of NaB revealed a significant reversal of NaB-induced cell death upon overexpression of either Glo1 or Stat3, further supporting the significance of Stat3 and Glo1 in the pro-apoptotic activity of NaB in DU145 cells.

Treatment with NaB also enhanced ROS production, possibly resulting from the inhibition of the antioxidant genes such as HO-1. Consistent with the results of a previous study in colorectal cancer (35), blocking ROS generation with NAC significantly increased Stat3 phosphorylation in NaB-treated DU145 cells. Therefore, the inhibition of Stat3 activity by NaB may be modulated by suppression of JAK2 activity and elevation of ROS production. Besides the antioxidant activity, HO-1 can promote cancer progression (36). Co-treatment with Colivelin remarkably increased HO-1 expression, suggesting a positive feedback loop between Stat3 and HO-1. Clinical observations indicate that Stat1, a tumor suppressor, may act as a reliable prognostic cancer marker (37). There exists a reciprocal regulation between Stat1 and Stat3, as inhibiting Stat3 activity increases Stat1 phosphorylation (38). Hence, the balance between the levels of Stat1 and Stat3 is considered to control the cell fate and cancer progression. Accordingly, it is possible that the anticancer activity of NaB in PCa cells may be associated with the increased expression of p-Stat1(Ser727).

The hormetic effect of MGO in cancer cells has been reported. At lower dose, MGO may be beneficial, while excessive MGO induces apoptosis in PCa (4). Given that MGO inhibits the Nrf2/HO-1 pathway in human umbilical vein endothelial cells (39), it was hypothesized that MGO may affect the viability and the expression of Nrf2, Glo1 and HO-1 in PCa cells. Consistently, treatment with MGO at high concentrations (>800 μM) greatly reduced the levels of Nrf2, Glo1 and HO-1, as well as the viability in DU145 cells. Thus, NaB-induced MGO generation subsequently diminished the expression of Nrf2, Glo1 and HO-1, leading to increased production of MGO and ROS, thereby further enhancing the anticancer effects of NaB.

Activation of CaMKII via ER stress is reported to trigger apoptotic cell death through multiple pathways, including (i) the JNK/Fas and ERK1/2-triggered apoptosis, (ii) mitochondrial membrane permeabilization caused by calcium uptake by mitochondria and the release of cytochrome c, and (iii) activation of p-Stat1 (Ser 727)-induced apoptotic signaling pathway (40). A novel finding is that NaB markedly increases the phosphorylation of CaMKII in DU145 cells. Interestingly, treatment with KN-93, a CaMKII inhibitor, remarkably reduced the production of MG-H1 in the absence or presence of NaB. Thus, the NaB-induced apoptosis may be, at least in part, due to CaMKII-mediated MGO production and the underlying mechanisms need further investigation. Under extracellular and intracellular stresses, the MAPKs, including ERK1/2, JNK and p38, are activated and subsequently, the pro-apoptotic

processes are initiated (41). Activation of JNK has been revealed to attenuate PCa progression by inducing apoptosis and inhibiting Nrf2 activity through the accumulation of nuclear Bach1 level (42,43). Because NaB-mediated activation of Stat1, MAPKs and pro-apoptotic proteins was strongly abolished by KN-93, CaMKII-induced apoptosis may be regulated by Stat1 and MAPKs-induced apoptotic responses. As anticipated, concurrent administration of Colivelin, KN-93, or NAC effectively counteracted NaB-induced death in DU145 cells. Collectively, these results suggested that the cytotoxic effect of NaB may be attributed to the inhibition of the Nrf2/Glo1/MGO pathway and Stat3, and increased CaMKII activation and ROS production.

The c-Myc and cyclin D1 are key mediators in promoting cell cycle progression, migration and proliferation (31). The results of the present study revealed that the levels of c-Myc and cyclin D1 in DU145 cells were markedly inhibited by NaB treatment. Thus, the inhibitory effects of NaB on cell proliferation and migration may be linked to the suppression of c-Myc/cyclin D1-regulated responses. In addition, the inhibition of cell proliferation by NaB was attenuated by KN-93, implicating the involvement of CaMKII in cell proliferation. Importantly, NaB treatment had no significant effects on the viability and the expression of Glo1 and Stat3 of RWPE-1 cells, indicating that the effects of NaB are specific for PCa cells. Despite significant advancements in the early detection, medical treatment and surgical castration of PCa, a large portion of patients will progress to advanced or metastatic CRPC within 2-3 years (44). It has been hypothesized that the androgen axis plays a pivotal role in the progression of CRPC. Numerous agents, including androgen receptor (AR) signaling inhibitors and CYP17A1 inhibitors, have been developed for the therapy of CRPC. However, these agents fail to suppress CRPC (45). The results of the present study confirmed that NaB significantly induces cell death and inhibits the proliferation and migration of DU145 cells, suggesting that NaB may attenuate CRPC progression.

In summary, it was demonstrated in the present study that the anticancer effect of NaB on DU145 cells may be through suppression of the Nrf2/Glo1 pathway via downregulation of the JAK2/Stat3 cascade, thereby accumulating cytotoxic MGO. Activation of CaMKII and MAPKs may also account for NaB-induced cell death, as illustrated in Fig. 6C. Taken together, NaB could serve as a potential therapeutic agent for CRPC.

Acknowledgements

The authors acknowledge the assistance and suggestions of Dr Yu-Chuan Huang of Instrument Center of National Defense Medical Center (Taipei, Taiwan, R.O.C.) on the instrument operation techniques.

Funding

The present study was partially supported by the Ministry of Science and Technology, Taiwan, R.O.C. (grant no. 108-2320-B-303-004-MY3).

Availability of data and materials

The datasets used and/or analyzed during the current study are available from the corresponding author on reasonable request.

Authors' contributions

ZML carried out the experiments and developed methodology. ZML, YJH and TZ analyzed, validated and curated the data. YJH and TCC designed and supervised the study. TCC wrote the manuscript. YJH and ZML confirm the authenticity of all the raw data. All authors read and approved the final version of the manuscript. The authors declare that all data were generated in-house and that no paper mill was used.

Ethics approval and consent to participate

Not applicable.

Patient consent for publication

Not applicable.

Competing interests

The authors declare that they have no competing interests.

References

1. Rawla P: Epidemiology of prostate cancer. World J Oncol 10: 63-89, 2019.
2. Liberti MV and Locasale JW: The warburg effect: How does it benefit cancer cells? Trends Biochem Sci 41: 211-218, 2016.
3. Monache SD, Pulcini F, Frosini R, Mattei V, Talesa VN and Antognelli C: Methylglyoxal-dependent glycative stress is prevented by the natural antioxidant oleuropein in human dental pulp stem cells through Nrf2/Glo1 pathway. Antioxidants (Basel) 10: 716, 2021.
4. Milanesa DM, Choudhury MS, Mallouh C, Tazaki H and Konno S: Methylglyoxal-induced apoptosis in human prostate carcinoma: Potential modality for prostate cancer treatment. Eur Urol 37: 728-734, 2000.
5. He Y, Zhou C, Huang M, Tang C, Liu X, Yue Y, Diao Q, Zheng Z and Liu D: Glyoxalase system: A systematic review of its biological activity, related-diseases, screening methods and small molecule regulators. Biomed Pharmacother 131: 110663, 2020.
6. Antognelli C, Mezzasoma L, Fettucciari K, Mearini E and Talesa VN: Role of glyoxalase I in the proliferation and apoptosis control of human LNCaP and PC3 cells. Prostate 73: 121-132, 2013.
7. Sakamoto H, Mashima T, Kizaki A, Dan S, Hashimoto Y, Naito M and Tsuruo T: Glyoxalase I is involved in resistance of human leukemia cells to antitumor agent-induced apoptosis. Blood 95: 3214-3218, 2000.
8. Pouremamali F, Pouremamali A, Dadashpour M, Soozangar N and Jeddi F: An update of Nrf2 activators and inhibitors in cancer prevention/promotion. Cell Commun Signal 20: 100, 2022.
9. Zhang HS, Du GY, Zhang ZG, Zhou Z, Sun HL, Yu XY, Shi YT, Xiong DN, Li H and Huang YH: NRF2 facilitates breast cancer cell growth via HIF1α-mediated metabolic reprogramming. Int J Biochem Cell Biol 95: 85-92, 2018.
10. Xue M, Rabbani N, Momiji H, Imbasi P, Anwar MM, Kitteringham N, Park BK, Souma T, Moriguchi T, Yamamoto M and Thornalley PJ: Transcriptional control of glyoxalase 1 by Nrf2 provides a stress-responsive defense against dicarbonyl glycation. Biochem J 443: 213-222, 2012.
11. Iurlaro R and Muñoz-Pinedo C: Cell death induced by endoplasmic reticulum stress. FEBS J 283: 2640-2652, 2016.
12. Cullinan SB, Zhang D, Hannink M, Arvisais E, Kaufman RJ and Diehl JA: Nrf2 is a direct PERK substrate and effector of PERK-dependent cell survival. Mol Cell Biol 23: 7198-7209, 2003.
13. Fujiki T, Ando F, Murakami K, Isobe K, Mori T, Susa K, Nomura N, Sohara E, Rai T and Uchida S: Tolvaptan activates the Nrf2/HO-1 antioxidant pathway through PERK phosphorylation. Sci Rep 9: 9245, 2019.
14. Lee H, Jeong AJ and Ye SK: Highlighted STAT3 as a potential drug target for cancer therapy. BMB Rep 52: 415-423, 2019.

15. Tian Y, Liu H, Wang M, Wang R, Yi G, Zhang M and Chen R: Role of STAT3 and NRF2 in tumors: Potential targets for antitumor therapy. Molecules 27: 8768, 2022.
16. Antognelli C, Gambelunghe A, Talesa VN and Muzi G: Reactive oxygen species induce apoptosis in bronchial epithelial BEAS-2B cells by inhibiting the antiglycation glyoxalase I defence: Involvement of superoxide anion, hydrogen peroxide and NF-κB. Apoptosis 19: 102-116, 2014.
17. McCoy F, Eckard L, Chen SL and Nutt LK: Metabolic regulation of apoptosis via Ca^{+}/Calmodulin Kinase II (CaMKII). BMC Proc 6(Suppl 3): P36, 2012.
18. He Q and Li Z: The dysregulated expression and functional effect of CaMK2 in cancer. Cancer Cell Int 21: 326, 2021.
19. Bridgeman SC, Northrop W, Melton PE, Ellison GC, Newsholme P and Mamotte CDS: Butyrate generated by gut microbiota and its therapeutic role in metabolic syndrome. Pharmacol Res 160: 105174, 2020.
20. Chen J, Zhao KN and Vitetta L: Effects of intestinal microbial-elaborated butyrate on oncogenic signaling pathways. Nutrients 11: 1026, 2019.
21. Gasparian A, Aksenova M, Oliver D, Levina E, Doran R, Lucius M, Piroli G, Oleinik N, Ogretmen B, Mythreye K, *et al*: Depletion of COPI in cancer cells: The role of reactive oxygen species in the induction of lipid accumulation, noncanonical lipophagy and apoptosis. Mol Biol Cell 33: ar135, 2022.
22. Jaud M, Philippe C, Van Den Berghe L, Ségura C, Mazzolini L, Pyronnet S, Laurell H and Touriol C: The PERK branch of the unfolded protein response promotes DLL4 expression by activating an alternative translation mechanism. Cancers (Basel) 11: 142, 2019.
23. Hur W, Sun Z, Jiang T, Mason DE, Peters EC, Zhang DD, Luesch H, Schultz PG and Gray NS: A small-molecule inducer of the antioxidant response element. Chem Biol 17: 537-547, 2010.
24. Lv C, Huang Y, Wang Q, Wang C, Hu H, Zhang H, Lu D, Jiang H, Shen R, Zhang W and Liu S: Ainsliadimer A induces ROS-mediated apoptosis in colorectal cancer cells via directly targeting peroxiredoxin 1 and 2. Cell Chem Biol 30: 295-307, 2023.
25. Xie JR, Chen XJ and Zhou G: Nuciferine inhibits oral squamous cell carcinoma partially through suppressing the STAT3 signaling pathway. Int J Mol Sci 24: 14532, 2023.
26. Pattison MJ, Mackenzie KF and Arthur JS: Inhibition of JAKs in macrophages increases lipopolysaccharide-induced cytokine production by blocking IL-10-mediated feedback. J Immunol 189: 2784-2792, 2012.
27. Mu D, Gao Z, Guo H, Zhou G and Sun B: Sodium butyrate induces growth inhibition and apoptosis in human prostate cancer DU145 cells by up-regulation of the expression of annexin A1. PLoS One 8: e74922, 2013.
28. Zhang X, Guo J, Wei X, Niu C, Jia M, Li Q and Meng D: Bach1: Function, regulation, and involvement in disease. Oxid Med Cell Longev 2018: 1347969, 2018.
29. Avalle L, Pensa S, Regis G, Novelli F and Poli V: STAT1 and STAT3 in tumorigenesis: A matter of balance. JAKSTAT 1: 65-72, 2012.
30. Guo Y, Zhang Y, Yang X, Lu P, Yan X, Xiao F, Zhou H, Wen C, Shi M, Lu J and Meng QH: Effects of methylglyoxal and glyoxalase I inhibition on breast cancer cells proliferation, invasion, and apoptosis through modulation of MAPKs, MMP9, and Bcl-2. Cancer Biol Ther 17: 169-180, 2016.
31. Chen H, Liu H and Qing G: Targeting oncogenic Myc as a strategy for cancer treatment. Signal Transduct Target Ther 3: 5, 2018.
32. Thulin MH, Määttä J, Linder A, Sterbova S, Ohlsson C, Damber JE, Widmark A and Persson E: Inhibition of STAT3 prevents bone metastatic progression of prostate cancer in vivo. Prostate 81: 452-462, 2021.
33. Kim SJ, Saeidi S, Cho NC, Kim SH, Lee HB, Han W, Noh DY and Surh YJ: Interaction of Nrf2 with dimeric STAT3 induces IL-23 expression: Implications for breast cancer progression. Cancer Lett 500: 147-160, 2021.
34. Rouillard AD, Gundersen GW, Fernandez NF, Wang Z, Monteiro CD, McDermott MG and Ma'ayan A: The harmonizome: A collection of processed datasets gathered to serve and mine knowledge about genes and proteins. Database (Oxford) 2016: baw100, 2016.
35. Kim DH, Park KW, Chae IG, Kundu J, Kim EH, Kundu JK and Chun KS: Carnosic acid inhibits STAT3 signaling and induces apoptosis through generation of ROS in human colon cancer HCT116 cells. Mol Carcinog 55: 1096-110, 2016.
36. Jagadeesh ASV, Fang X, Kim SH, Guillen-Quispe YN, Zheng J, Surh YJ and Kim SJ: Non-canonical vs. Canonical functions of heme oxygenase-1 in cancer. J Cancer Prev 27: 7-15, 2022.
37. Zhang J, Wang F, Liu F and Xu G: Predicting STAT1 as a prognostic marker in patients with solid cancer. Ther Adv Med Oncol 12: 1758835920917558, 2020.
38. Regis G, Pensa S, Boselli D, Novelli F and Poli V: Ups and downs: The STAT1:STAT3 seesaw of interferon and gp130 receptor signalling. Semin Cell Dev Biol 19: 351-359, 2008.
39. Wang G, Wang Y, Yang Q, Xu C, Zheng Y, Wang L, Wu J, Zeng M and Luo M: Metformin prevents methylglyoxal-induced apoptosis by suppressing oxidative stress in vitro and in vivo. Cell Death Dis 13: 29, 2022.
40. Timmins JM, Ozcan L, Seimon TA, Li G, Malagelada C, Backs J, Backs T, Bassel-Duby R, Olson EN, Anderson ME and Tabas I: Calcium/calmodulin-dependent protein kinase II links ER stress with Fas and mitochondrial apoptosis pathways. J Clin Invest 119: 2925-2941, 2009.
41. Yue J and López JM: Understanding MAPK signaling pathways in apoptosis. Int J Mol Sci 21: 2346, 2020.
42. Xu R and Hu J: The role of JNK in prostate cancer progression and therapeutic strategies. Biomed Pharmacother 121: 109679, 2020.
43. Kanzaki H, Shinohara F, Itohiya K, Yamaguchi Y, Katsumata Y, Matsuzawa M, Fukaya S, Miyamoto Y, Wada S and Nakamura Y: RANKL induces Bach1 nuclear import and attenuates Nrf2-mediated antioxidant enzymes, thereby augmenting intracellular reactive oxygen species signaling and osteoclastogenesis in mice. FASEB J 31: 781-792, 2017.
44. Harris WP, Mostaghel EA, Nelson PS and Montgomery B: Androgen deprivation therapy: Progress in understanding mechanisms of resistance and optimizing androgen depletion. Nat Clin Pract Urol 6: 76-85, 2009.
45. Chandrasekar T, Yang JC, Gao AC and Evans CP: Mechanisms of resistance in castration-resistant prostate cancer (CRPC). Transl Androl Urol 4: 365-380, 2015.